THE SPIN OF THE 2·78 MeV STATE OF ^{19}Ne

By D. J. Baugh,* J. Nurzyński,* D. M. Rosalky,* and C. H. Osman*

[*Manuscript received February* 21, 1969]

Summary

The ^{20}Ne(^{3}He, α)^{19}Ne reaction was studied at 10 and 15 MeV bombarding energy. A DWBA analysis was performed indicating an $l = 4$ or $l = 5$ transition to the 2·78 MeV state in ^{19}Ne.

I. Introduction

There has been considerable theoretical work done on the low lying levels of ^{19}F, which have been successfully described in terms of the shell model (Elliott and Flowers 1955; Redlich 1955), the strong coupling collective model (Paul 1957; Rakavy 1957; Chi and Davidson 1963), and the SU$_3$ classification of states (Elliott 1958; Harvey 1964). All these models predict that the isolated level at 2·79 MeV should have a spin $\frac{9}{2}$+. The experimental evidence (Allen *et al.* 1965; Olness and Wilkinson 1966) at the time this work was completed limited the spin of this state to $\frac{5}{2}$ or $\frac{9}{2}$ with $\frac{9}{2}$ favoured, the parity being undetermined. Recently triple correlation and lifetime measurements have been published (Tolbert, Cockburn, and Prosser 1968) which determined the spin and parity of this state to be $\frac{9}{2}$+. The mirror nucleus ^{19}Ne has a very similar level structure to that of ^{19}F (Fig. 1) and, since in both ^{19}F and ^{19}Ne the level in question is isolated, a direct equivalence can be made between the 2·78 MeV level in ^{19}Ne and the 2·79 MeV level in ^{19}F. This conclusion is supported by the limited data (Olness, Poletti, and Warburton 1967) on the γ decay of ^{19}Ne with that of ^{19}F.

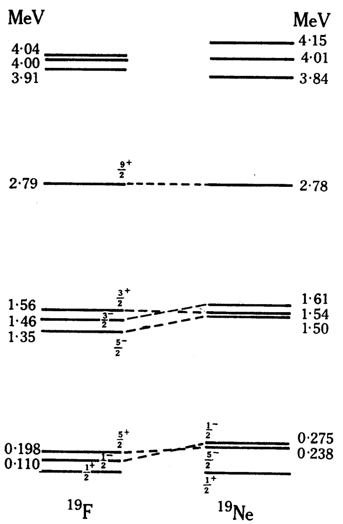

Fig. 1.—Energy level diagrams for the mirror nuclei ^{19}F and ^{19}Ne.

In order that an attempt could be made to distinguish between a $\frac{5}{2}$ and a $\frac{9}{2}$ assignment for the 2·78 MeV state in ^{19}Ne, measurements of the ^{20}Ne(^{3}He, α)^{19}Ne reaction were taken. The target consisted of a gas cell containing enriched ^{20}Ne gas. The energy resolution was limited by straggling through the windows of the cell, and consequently only the ^{3}He elastic scattering and the α-particle groups corresponding to the ground and 2·78 MeV states in ^{19}Ne could be adequately resolved. Angular distributions of these three groups were measured at 10 MeV and of the elastic scattering and 2·78 MeV α-particle group at 15 MeV bombarding energy.

* Research School of Physical Sciences, Australian National University, Canberra, A.C.T. 2600.

II. Optical Model Analysis of the Elastic Scattering

The 10 and 15 MeV elastic scattering data were analysed using a standard optical potential $V(r)$ with Saxon–Woods form factors for both the real and imaginary parts:

$$V(r) = -U[1+\exp\{(r-r_0 A^{\frac{1}{3}})/a_0\}]-\mathrm{i}W[1+\exp\{(r-r_i A^{\frac{1}{3}})/a_i\}]+V_{\mathrm{C}},$$

where V_{C} was the Coulomb potential due to a uniformly charged sphere of radius $1\cdot 3 A^{\frac{1}{3}}$.

Table 1

optical model potentials for ^{3}He and α-particles scattered by ^{20}Ne

Type of Potential	U (MeV)	r_0 (f)	a_0 (f)	W (MeV)	r_i (f)	a_i (f)	Potential Number
10 MeV ^{3}He	133·1	1·10	0·788	8·955	1·919	0·390	1
	126·7	1·15	0·764	9·066	1·910	0·353	2
	120·6	1·20	0·740	9·136	1·904	0·316	3
	114·8	1·25	0·715	9·174	1·905	0·272	4
	195·3	1·10	0·739	10·698	1·912	0·323	5
	185·3	1·15	0·716	10·813	1·910	0·291	6
	176·0	1·20	0·694	10·876	1·912	0·255	7
	167·3	1·25	0·672	10·949	1·917	0·216	8
15 MeV ^{3}He	123·4	1·10	0·772	10·964	1·836	0·896	9
	116·5	1·15	0·755	11·418	1·800	0·916	10
	110·2	1·20	0·737	11·949	1·758	0·930	11
	104·5	1·25	0·715	12·699	1·701	0·961	12
	186·6	1·10	0·708	15·833	1·591	0·993	13
	176·2	1·15	0·690	17·107	1·522	1·021	14
	166·7	1·20	0·671	18·783	1·437	1·056	15
	157·9	1·25	0·650	21·151	1·325	1·102	16
15 MeV alpha	202·4	1·867	0·440	11·661	1·867	0·440	

A two-dimensional grid search was made in which U and r_0 were changed between 100 and 200 MeV in steps of 10 MeV and between 1·10 and 1·25 f in steps of 0·05 f respectively. At each grid point the four remaining parameters (a_0, W, r_i, and a_i) were varied freely until the fit between theory and experiment was optimized. For both the 10 and 15 MeV data two optimum fits in the range $U = 100$–200 MeV were found for each value of r_0. The grid search only determined the value of U for a given value of r_0 to the nearest 10 MeV and, therefore, starting from the optimum parameters obtained from the grid search a five-parameter optimization (U, a_0, W, r_i, and a_i) was performed. The resulting parameters which display both discrete and continuous ambiguities are quoted in Table 1. These potentials were used as the entrance channel distorting potentials in the DWBA analysis of the (^{3}He, α) data. The optical potential for the exit (α-particle) channel (Table 1) was obtained from the analysis of measurements of 14·96 MeV α-particles scattered by ^{20}Ne (Bourke, personal communication).

III. DWBA Analysis of the (^{3}He, α) Data

For the 10 MeV incident energy ground state α-particle group ($l = 0$), zero range, no-cutoff DWBA calculations were done using the appropriate potentials of Table 1. The calculated curves were, as usual, multiplied by an arbitrary normalization factor containing the overlap of the internal wave functions of free ^{3}He and α-particles and the experimental spectroscopic factor S_{lj}. Satisfactory fits could only be obtained with the entrance channel potentials labelled 1–4 in Table 1. The quality of the fit was not sensitive to which of these potentials was used.

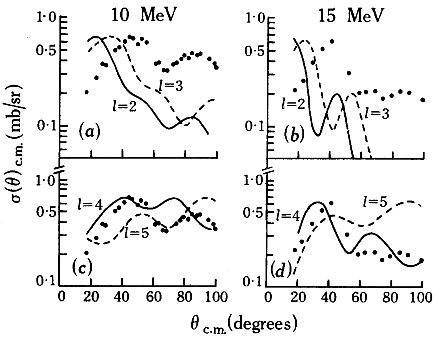

Fig. 2.—DWBA fits for $l = 2$, 3, 4, and 5 to the 10 and 15 MeV ^{3}He data for the reaction ^{20}Ne(^{3}He, α)^{19}Ne leading to the 2·78 MeV state in ^{19}Ne.

For the group leading to the 2·78 MeV state, zero range, no-cutoff calculations were performed for values of the angular momentum transfer $l = 2$, 3, 4, and 5. The α-particle potential of Table 1 was used throughout in the exit channel, and the potentials 1–8 and 9–16 of Table 1 were used for the 10 MeV and 15 MeV data respectively in the ^{3}He channel. None of the l values and none of the entrance channel potentials 5–8 and 13–16 gave acceptable fits to the data. The calculations using the potentials 1–4 and 9–12 were insensitive to the value of r_0 and, therefore, all calculations discussed henceforth used potentials 3 and 11 for the 10 MeV and 15 MeV reactions respectively. The results are compared with the experimental data in Figure 2. For the $l = 2$ and $l = 3$ calculations at both 10 and 15 MeV (Figs 2(*a*) and 2(*b*)) the first maximum of the calculated distribution occurred at too small an angle compared with that of the experimental data and the calculated distributions fell off too rapidly with angle. For $l = 4$ (Figs 2(*c*) and 2(*d*)) the shapes of the calculated distributions reflected more accurately those of the experiment. At both 10 and 15 MeV the position of the first maximum in the theoretical cross section was, however, at an angle 6°–8° smaller than that of the experiment. For $l = 5$ the shapes of the theoretical distributions represent the data less well than the $l = 4$ distributions and the first maximum is at slightly too large an angle (5° and 2°–3° for 10 MeV and 15 MeV respectively).

Small readjustments of the exit channel parameters were considered justified since problems associated with the nondirect contributions to the α-particle elastic scattering, with angular momentum mismatch, and with the nonsurface nature of (^{3}He, α) reactions make the assumption that an optical model analysis of the elastic scattering α-particle data accurately "measures" the exit channel parameters doubtful (Stock *et al.* 1967). For $l = 2$, 3, 4, and 5, and for both 10 and 15 MeV bombarding energy, calculations were made in which the depths of the real and imaginary α-particle potential were varied between the limits 180 and 220 MeV and 4 and 20 MeV respectively. For $l = 2$ this procedure did not significantly improve the fit to either the 10 MeV or 15 MeV data. For $l = 3$ an improvement in the fit to the 10 MeV data could be obtained by reducing the imaginary potential depth to about 4 MeV. This improvement was in the general slope and shape of the predicted distribution. The fit was still poor however, the first maximum in the theoretical cross section being approximately 13° out of phase with that of the experimental data. For $l = 3$ and 15 MeV incident energy, adjustment of the exit channel parameters did not significantly improve the agreement between theory and experiment. For $l = 4$ and $l = 5$, fits to the 10 and 15 MeV data resulting from a readjustment of the real and imaginary α-particle depths are shown in Figure 3.

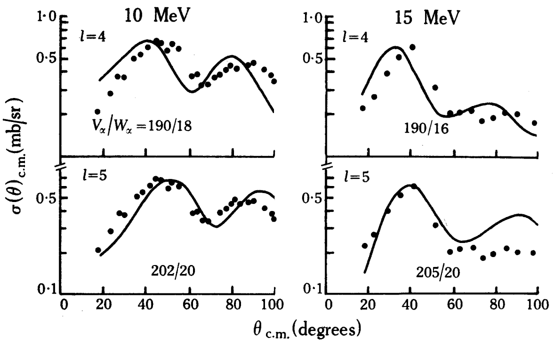

Fig. 3.—DWBA fits for $l = 4$ and 5 to the 10 and 15 MeV ^{3}He data for the reaction ^{20}Ne(^{3}He, α)^{19}Ne leading to the 2·78 MeV state in ^{19}Ne obtained by readjusting the potential depths V_α and W_α in the exit channel. The readjusted values of V_α/W_α are indicated for each curve.

Whilst the fits displayed in Figure 3 are not entirely adequate, they are significantly better than the $l = 2$ and $l = 3$ fits, and allow the conclusion that the angular momentum transfer l is not $l = 2$ or $l = 3$. Since a $\frac{5}{2}$ or $\frac{9}{2}$ spin assignment limits the possible l values to 2, 3, 4, or 5, the exclusion of $l = 2$ and $l = 3$ enabled the angular momentum transfer for the transition to the 2·78 MeV state in ^{19}Ne to be assigned the value $l = 4$ or $l = 5$. Provided the correspondence between the 2·78 MeV state in ^{19}Ne and the 2·79 MeV state in ^{19}F is assumed, therefore, the spin of the 2·78 MeV state in ^{19}Ne is $\frac{9}{2}$.

IV. References

Allen, J. P., Howard, A. J., Bromley, D. A., and Olness, J. W. (1965).—*Phys. Rev.* **140**, B1245.

Chi, B. E., and Davidson, J. P. (1963).—*Phys. Rev.* **131**, 366.

Elliott, J. P. (1958).—*Proc. R. Soc.* A **245**, 128.

Elliott, J. P., and Flowers, B. H. (1955).—*Proc. R. Soc.* A **229**, 536.

Harvey, M. (1964).—*Nucl. Phys.* **52**, 542.

Olness, J. W., Poletti, A. R., and Warburton, E. K. (1967).—*Phys. Rev.* **161**, 1131.

Olness, J. W., and Wilkinson, D. H. (1966).—*Phys. Rev.* **141**, 966.

Paul, E. B. (1957).—*Phil. Mag.* **15**, 311.

Rakavy, G. (1957).—*Nucl. Phys.* **4**, 375.

Redlich, M. G. (1955).—*Phys. Rev.* **99**, 1427.

Stock, R., Bock, R., David, P., Duhm, H. H., and Tamura, T. T. (1967).—*Nucl. Phys.* A **104**, 136.

Tolbert, D. D., Cockburn, P. M., and Prosser, F. W. (1968).—*Phys. Rev. Lett.* **21**, 1535.